



**HAL**  
open science

## **Bis(monoacylglycero)phosphate regulates oxysterol binding protein-related protein 11 dependent sterol trafficking**

Maud Arnal-Levron, Yinan Chen, Peter Greimel, Federica Calevro, Karen Gaget, Fabien Riols, Aurélie Batut, Justine Bertrand-Michel, Françoise Hullin-Matsuda, Vesa Olkkonen, et al.

► **To cite this version:**

Maud Arnal-Levron, Yinan Chen, Peter Greimel, Federica Calevro, Karen Gaget, et al.. Bis(monoacylglycero)phosphate regulates oxysterol binding protein-related protein 11 dependent sterol trafficking. *Biochimica et Biophysica Acta Molecular and Cell Biology of Lipids*, 2019, 1864 (9), pp.1247-1257. 10.1016/j.bbalip.2019.05.011 . hal-02146150

**HAL Id: hal-02146150**

**<https://hal.science/hal-02146150>**

Submitted on 26 Oct 2021

**HAL** is a multi-disciplinary open access archive for the deposit and dissemination of scientific research documents, whether they are published or not. The documents may come from teaching and research institutions in France or abroad, or from public or private research centers.

L'archive ouverte pluridisciplinaire **HAL**, est destinée au dépôt et à la diffusion de documents scientifiques de niveau recherche, publiés ou non, émanant des établissements d'enseignement et de recherche français ou étrangers, des laboratoires publics ou privés.



Distributed under a Creative Commons Attribution - NonCommercial 4.0 International License

**Bis(monoacylglycerol)phosphate regulates oxysterol binding protein-related protein 11 dependent sterol trafficking**

Maud Arnal-Levron<sup>1</sup>, Yinan Chen<sup>1</sup>, Peter Greimel<sup>2</sup>, Federica Calevro<sup>3</sup>, Karen Gaget<sup>3</sup>, Fabien Riols<sup>4</sup>, Aurélie Batut<sup>4</sup>, Justine Bertrand-Michel<sup>4</sup>, Françoise Hullin-Matsuda<sup>1</sup>, Vesa M. Olkkonen<sup>5</sup>, Isabelle Delton<sup>1</sup> and Céline Luquain-Costaz<sup>1</sup>

<sup>1</sup>*Inserm, U1060, CarMeN Laboratory, Villeurbanne, France; INSA-Lyon, Villeurbanne, France*

<sup>2</sup>*Lipid Biology Laboratory, RIKEN, 2-1, Hirosawa, Wako-shi, Saitama 351-0198, Japan*

<sup>3</sup>*UMR203 BF2I, INRA, INSA de Lyon, Villeurbanne, France*

<sup>4</sup>*Inserm U1048, Toulouse, France; Lipidomic Core Facility, Metatoul Platform, Université de Toulouse, Université Paul Sabatier, Toulouse, France*

<sup>5</sup>*Minerva Foundation Institute for Medical Research, Biomedicum 2U, FI-00290 Helsinki, Finland*

To whom correspondence should be addressed: Céline Luquain-Costaz, UMR 1060 INSERM, INSA-Lyon, IMBL Building, 20 Ave A. Einstein, 69621 Villeurbanne, France. Tel: 33-4-72-43-72-36; Fax: 33-4-72-43-85-24. E-mail: [celine.costaz@insa-lyon.fr](mailto:celine.costaz@insa-lyon.fr)

**Keywords:** Bis(monoacylglycerol)phosphate, macrophages, cholesterol, oxysterols, late endosome, oxysterol binding protein

---

Abbreviations: 7 $\beta$ -OH 7 $\beta$ -hydroxycholesterol; 7-keto, 7-ketocholesterol; ABCA1, ATP-binding cassette A1, ABCG1, ATP-binding cassette G1 BMP, bis(monoacylglycerol)phosphate; CE, cholesterol ester; ER, endoplasmic reticulum; FC, free cholesterol; LE, late endosome; LXR, liver X receptor; NPC, Niemann Pick disease type C; MCS, membrane contact sites; OSBP, oxysterol binding protein; ORP, OSBP-related protein; PG, phosphatidylglycerol; PS, phosphatidylserine; PI4P, phosphatidylinositol-4-phosphate; PIP2, phosphatidylinositol 4,5 diphosphate.

---

**Abstract**

Bis(Monoacylglycerol)Phosphate (BMP) is a unique phospholipid localized in late endosomes, a critical cellular compartment in low density lipoprotein (LDL)-cholesterol metabolism. In previous work, we demonstrated the important role of BMP in the regulation of macrophage cholesterol homeostasis. BMP exerts a protective role against the pro-apoptotic effect of oxidized LDL (oxLDL) by reducing the production of deleterious oxysterols. As the intracellular sterol traffic in macrophages is in part regulated by oxysterol binding protein (OSBP) and OSBP-related proteins (ORPs), we investigated the role of ORP11, localized at the Golgi-late endosomes interface, in the BMP-mediated protection from oxLDL/oxysterol cytotoxicity. Stably silencing of ORP11 in mouse RAW264.7 macrophages via a shRNA lentiviruses system had no effect on BMP production. However, ORP11 knockdown abrogated the protective action of BMP against oxLDL induced apoptosis. In oxLDL treated control cells, BMP enrichment was associated with reduced generation of 7-oxysterols, while these oxysterol species were abundant in the ORP11 knock-down cells. Of note, BMP enrichment in ORP11 knock-down cells was associated with a drastic increase in free cholesterol and linked to a decrease of cholesterol efflux. The expression of ATP-binding cassette-transporter G1 (*ABCG1*) was also reduced in the ORP11 knock-down cells. These observations demonstrate a cooperative function of ORP11 and BMP, in intracellular cholesterol trafficking in cultured macrophages. We suggest that BMP favors the egress of cholesterol from late endosomes via an ORP11-dependent mechanism, resulting in a reduced production of cytotoxic 7-oxysterols.

## 1. Introduction

Oxysterols are found enriched in pathologic structures such as macrophage foam cells and atherosclerotic lesions [1]. They originate from a massive uptake of oxLDL-containing oxysterols in subendothelial macrophages. Moreover, macrophages are able to produce oxysterols intracellularly in late endosomes (LE), from both LDL-associated and cellular cholesterol [2]. The large family of oxysterols includes sterols oxidized at the ring, mainly at carbon 7 (e.g., 7-ketocholesterol and 7 $\alpha$ / $\beta$ -hydroxycholesterol) and those oxidized at the side-chain, such as 24S-hydroxycholesterol, 25-hydroxycholesterol, and 27-hydroxycholesterol. Generally, ring-oxidized sterols tend to be formed non-enzymatically, whereas side-chain oxidation is usually catalyzed by specific enzymes belonging to the cytochrome P450 family. The bulk of oxysterols in oxLDL are oxidized at carbon 7, such as 7 $\beta$ -hydroxycholesterol (7 $\beta$ -HC) and 7-ketocholesterol (7-keto). These oxysterols are responsible for the ability of oxLDL to induce cellular oxidative stress and cytotoxicity, mainly *via* apoptosis [3–6].

Oxysterols are associated with a large variety of cellular effectors linked to atherosclerosis. Among them, oxysterol-binding protein (OSBP) and OSBP-related proteins (ORPs) constitute a family of lipid binding/transfer proteins conserved in eukaryotes [7–9]. Several reports have addressed the role of ORPs in intracellular cholesterol trafficking and homeostasis, for example : control of endoplasmic reticulum-late endosomes (ER –LE) contacts and LE motility (ORP1L), neutral lipid metabolism (ORP2), cholesterol egress from LE (ORP5), macrophage lipid and high-density lipoprotein metabolism (ORP8), apolipoprotein B-100 secretion (ORP10), and adipogenesis (ORP11) [10–12]. The silencing of ORP8 or ORP1L altered the lipidome in RAW macrophages emphasizing their important role in cellular lipid homeostasis [13].

Another important effector of oxysterols is bis(monoacylglycero)phosphate (BMP), a phospholipid preferentially found in LE membranes. BMP participates in cholesterol metabolism/trafficking in macrophages and regulates cholesterol efflux to HDL [5,14–17]. We recently showed that BMP exerts a protective action against the pro-apoptotic effect of oxLDL *via* a reduced production of intracellular oxysterols [5], but the underlying molecular mechanism remains to be characterized. However, the emerging roles of OSBP/ORPs in sterol trafficking between organelles suggest their putative involvement. BMP has already been linked to two key proteins implicated in intracellular cholesterol traffic, Niemann-Pick C1 (NPC1) and C2 (NPC2) that are mutated in the Niemann-Pick disease type C [18]. NPC1 and NPC2 are required to deliver free cholesterol from the endosomal compartment to the plasma membrane and ER [19,20]. *In vivo* NPC cells are characterized by aberrant BMP accumulation and oxidative stress [15]. Additionally, BMP and NPC2 cooperatively stimulate the efflux of cholesterol from the endosomal system [21–23].

In the present study, we focused on the concerted effect of BMP and members of the ORP family to protect against oxLDL cytotoxicity. ORP transcription level analysis identified ORP11 as the most promising candidate. Indeed, ORP11 not only localizes to the Golgi-LE interface [24] but also a strong association of *Osbp11* gene polymorphisms with cardiovascular risk factors and diabetes has been reported [25]. We stably silenced ORP11 in RAW264.7 macrophages and demonstrated that ORP11 knockdown abolished the protective effect of BMP by impairing BMP-induced egress of cholesterol/oxysterols from endosomal compartments. Our results suggest a functional interplay of BMP and ORP11 to protect macrophages from oxLDL-induced cytotoxicity, with implications for atherogenesis.

## **2. Materials and methods**

### *2.1. Cell culture and treatments*

RAW 264.7 cells were cultured in MEM supplemented with non-essential amino acids, 10% foetal bovine serum, 2 mM L-glutamine, 100 units/ml penicillin and 100 µg/ml streptomycin. They were routinely grown in T-75 flasks at 37°C in an atmosphere of 5% CO<sub>2</sub> and subcultured by trypsination at a 1:5 ratio. Experiments were started 24 h after seeding by pre-incubation without (control) or with 30 µM dioleoylphosphatidylglycerol (DOPG) liposomes (BMP-enriched) [26] for 24 h. The addition of PG was maintained throughout the experiments. Cells were then incubated in basal conditions (unloaded) or in presence of native (nLDL) or oxLDL (loaded) for 24h at physiological concentrations (100-200 µg/ml). Incubations with LDL were done in medium-containing 5% lipoprotein deficient serum (LPDS). Other details of incubation conditions are given below and/or in the figure legends. 293FT cells used for packaging of lentiviruses were cultured in Opti-MEM supplemented with 10% FBS and 1% GlutaMAX. They were grown in T-75 flasks at 37°C in an atmosphere of 5% CO<sub>2</sub>. Transfections were carried out at 24 h after seeding the cells in serum-free Opti-MEM GlutaMAX.

### *2.2. Preparation of lentiviruses and infection of RAW264.7 cells*

Short hairpin RNA (shRNA) encoding pLKO.1 lentiviral transfer vectors were purchased from Thermo Scientific TRC (The RNAi Consortium) or from Sigma MISSION<sup>®</sup> TRC-Mm 1.0 (Mouse) shRNA library (Sigma-Aldrich, St. Louis, MO, USA). After plating and selecting bacteria, a plasmid purification (Plasmid Midi Kit, Qiagen) and DNA quantification (NanoDrop<sup>®</sup>) were performed. A transfection complex was prepared using 4 µg shRNA transfer vector, 3 µg packaging plasmid p8.91 and 2 µg VSV-G expressing plasmid pMD2.G. This complex was transfected into 293FT packaging cells using FuGENE HD transfection reagent (Roche) in a 5:2 reagent:DNA proportion. After two days, viral supernatants were collected, filtered and used to infect RAW 264.7 cells. Lentiviral transduction was performed using 8 µg/ml hexadimethrine bromide and selection was carried out using puromycin 10 µg/ml. The silencing efficiency of five ORP11 targeting shRNA (shORP11) constructs was determined by quantitative real-time RT-PCR and the shRNA with the best silencing efficiency was selected for the following experiments. ORP3-specific shRNA lentivirus [13] was included for a comparison, and a non-target shRNA (shNT) SHC002V was used as a control plasmid. Early passages of the cell pools (until P8) were used for experiments, at which time no significant reduction in the silencing efficiency was observed.

### *2.3. Lipoprotein preparation and oxidation*

Human LDLs were isolated from plasma by sequential ultracentrifugation [27]. LDL oxidation was achieved during 5h dialysis at 37°C against 10 mM Tris, 150 mM NaCl, pH 7.4 supplemented with 10 µM of CuSO<sub>4</sub>. Subsequent overnight dialysis was performed at 4°C against 10 mM Tris, 150 mM NaCl, pH 7.4, containing 2 mM EDTA to eliminate CuSO<sub>4</sub> and stop oxidation. LDL oxidation was evaluated by GC-MS/MS quantification of their associated oxysterols compared to native LDL.

### *2.4. Evaluation of cytotoxicity*

After treatment, cells were washed with PBS and their viability was assessed using a colorimetric MTT assay (Cell proliferation Kit I, Roche) according to the manufacturer's instructions. MTT cleavage was determined by reading the absorbance at 560 nm. Cell

viability in control and BMP enriched-cells was expressed as the percentage of maximum cell viability relative to unloaded-control cells.

### *2.5. Extraction of RNA and proteins*

After treatment, RNA and proteins for ORPs analysis were extracted from cell lysates using NucleoSpin RNA/Protein kit (Macherey Nagel), according to manufacturer's instructions. For *ABCG1* and *LXR $\alpha$*  mRNA analysis, total RNA was isolated using Trizol reagent (Invitrogen) according to manufacturer's instructions. RNA concentrations were determined with a NanoDrop® spectrophotometer and protein concentrations estimated with a Qubit® fluorometer.

### *2.6. ORPs mRNA analysis*

For each RNA sample, the respective cDNA first-stand was generated with SuperScript® VILO cDNA Synthetis kit (Invitrogen) according to manufacturer's instructions. Each cDNA sample was amplified in triplicate for the genes of interest, using mouse *36B4* as a normalization gene in each run. Quantitative real-time RT-PCR reactions were performed using the Light Cycler® 480 SYBR Green I Master (Roche). The threshold was set in the linear range of fluorescence, and a threshold cycle (Ct) was measured for each well. The data was analyzed according to the comparative Fit Points method. The silencing efficiencies were evaluated by comparing the expression levels between the control (shNT) cells and the cell pool of interest. Primers are available on request.

### *2.7. ABCG1 and ABCA1 mRNAs analysis*

Total RNAs were treated with RQ1 RNase-Free DNase I (Promega Corporation, Madison, WI, USA), and reverse-transcribed with the SuperScript™ III First-Strand Synthesis System (Life Technologies, Carlsbad, CA, USA), using Oligo(dT) primers (Invitrogen by Life Technologies,) in order to obtain first-strand cDNA. The quality of the cDNA synthesized was examined by PCR. As a negative control, the remainder of the DNase treated RNA was examined by PCR using the same conditions. Quantitative real-time RT-PCR reactions were performed on a LightCycler® 480 Real-Time PCR System (Roche, Penzberg, Germany) using 1:2.5 diluted cDNAs and a LightCycler® 480 SYBR Green I Master Mix (Roche, Penzberg, Germany) according to manufacturer's instructions. For each gene, triplicate assays were performed. Two normalization gene candidates (*GAPDH* and *HPRT*) were tested for gene expression variation in all the experimental conditions used in this work. The *HPRT* gene was employed as a normalization gene as it met the criteria imposed by the BestKeeper software analysis (data not shown). The primer sequences are available on request.

### *2.8. Western Blot analysis*

ORP11 protein was electrophoresed on 6% polyacrylamide gels. After blocking unspecific binding, antibody incubations were carried out in blocking buffer (5% fat-free powdered milk in TBS containing 0.05% Tween 20). The bound primary antibodies were visualized with peroxidase-conjugated anti-rabbit IgG (Bio-Rad). Rabbit polyclonal antibody against ORP11 [24] was used at 1:800 dilution and mouse polyclonal antibody against tubulin (Sigma) at 1:1000 dilution. All data was quantified with ImageJ software.

### *2.9. Immunofluorescence*

Cells were plated on coverslips and, after treatments, fixed at room temperature for 30 min with 4% paraformaldehyde. Subsequently, cells were incubated for 30 min at room temperature with 0.1% BSA to block unspecific antibody binding and for 60 min with primary antibodies (anti-BMP, anti-ORP11 or anti-GM130) in PBS containing 0.05% saponin, followed by incubation with Alexa 488- or Alexa 546-conjugated secondary

antibodies. The specimens were mounted with Mowiol and examined with a Zeiss LSM 510 confocal microscope equipped with the C-Apochromat 63XW Korr (1.2 n.a.) objective. The data was quantified with ImageJ software using JACoP (Just Another Colocalization Plugin). Colocalization scores using Mander's overlap coefficient (M1 and M2) were calculated for individual cells representative of a cell population. Thresholds were set to remove the background signal while remaining representative of the confocal image.

#### *2.10. Incorporation of [<sup>3</sup>H]oleate into CE*

Macrophages were exposed to 1  $\mu$ Ci/ml [<sup>3</sup>H]oleate during 24 h of nLDL or oxLDL loading. Unloaded macrophages were labeled by suspending [<sup>3</sup>H]oleate into the growth medium utilizing an ethanolic stock solution, while maintaining final ethanol concentration <0.1%. After treatments, total lipids were extracted from cell lysates according to the method of Bligh and Dyer [28], separated by TLC (hexane/diethyl ether/acetic acid, 80:20:1, v/v) and quantified with a radioactivity analyzer (Raytest, France). Degree of cholesterol esterification was expressed as percentage of cholesteryl [<sup>3</sup>H]oleate relative to total radioactivity recovered.

#### *2.11. Sterol efflux to HDL*

Cells were pre-incubated with 2  $\mu$ Ci/ml [<sup>3</sup>H]cholesterol for 24 h. Sterol efflux under 6 h was measured in basal conditions (5% LPDS) or in response to HDL (100  $\mu$ g/ml) in 5% LPDS-containing medium. The total radioactivity in cells and in media was determined by liquid scintillation counting. Total lipids from both cell and media were extracted according to the method of Bligh and Dyer [28] and sterols were separated by TLC (hexane/diethyl ether/acetic acid/methanol, 50:50:1:5, v/v). The radioactivity associated with each sterol fraction (cholesterol and oxysterols, free or esterified) was measured with a radioactivity analyzer (Rayster, France) and converted to DPM according to liquid scintillation counting. The efflux of each sterol was expressed as the percentage of radioactivity released into the medium relative to total radioactivity in cells plus media.

#### *2.12. Quantification of BMP and PG species by LC-MS/MS*

After treatments, samples were spiked with C14:0/C14:0-BMP (DMBMP) and C14:0/C14:0-PG (DMPG) as internal standards, and total lipids were extracted from cell lysates and media according to the method of Bligh and Dyer (24). The resulting samples were dried under nitrogen flow and resuspended in methanol prior to measurement. LC-MS/MS was carried out on an Agilent 1100 Series HPLC system (Agilent Technologies, Santa Clara, CA) integrated with an 4000 QTrap mass spectrometer (AB SCIEX, Foster City, CA) using a Shiseido CAPCELL PAK C18 MGIII Type column (5 $\mu$ m, 2.0 x 50mm) (Shiseido CO., LTD., Tokyo, Japan). LC separation (2  $\mu$ l sample injection) was performed utilizing methanol:acetonitrile (95:5) with 25 mM ammonium formate and 0.1% formic acid as monocratic mobile phase at a flow rate of 100 $\mu$ l/min. The mass spectrometer was operated in positive ion mode utilizing the following optimized parameters for BMP and PG for multi reaction monitoring (MRM) mode: declustering potential 55V (for BMP) and 70V (for PG), collision energy 30V, collision cell exit potential 15V, entrance potential 10V, Q1 resolution set to unit and Q3 resolution set to low. Internal standards for quantification were monitored at 684.6/285.1 Da (for DMBMP) and at 684.6/495.5 Da (for DMPG).

#### *2.13. Quantification of total oxysterols by GC-MS*

Oxysterol were quantified by a modified protocol based on Iuliano [29]. After treatments, each cell pellet was crushed with a FastPrep <sup>®</sup>-24 Instrument (MP Biomedical) in Methanol/EGTA (2:1, v/v) solution. Total lipids were extracted by a modified method of Bligh and Dyer [28] from cell lysates and media in dichloromethane/methanol/water

(2.5:2.5:2, v/v), spiked with internal standards 19-hydroxycholesterol and vitamin E. Esters were hydrolyzed with KOH-CH<sub>2</sub>Cl<sub>2</sub> and neutralized with phosphoric acid addition prior to a second Bligh and Dyer extraction. Next, a Solid Phase Extraction (SPE) using SiOH 96-well plate (100 mg/well, Macherey Nagel) was performed. After sample application, the extraction plate was washed with 2-propranol/heptane (0.5:99.5, v/v) to eliminate neutral lipids like cholesterol. After drying under aspiration, oxysterols were eluted with 2-propranol/heptane (0.3:0.7, v/v). Oxysterols were converted to trimethylsilyl ether by addition of BSTFA/ACN (bis(trimethylsilyl)trifluoroacetamide/acetonitrile, 1:1; v:v) at 55°C for 60 min. Gas chromatography-mass spectrometric analysis was performed on a ThermoScientific Trace GC coupled to a Trace ISQ Mass selective detector (ThermoScientific). The silylated oxysterols were separated on an Agilent J&W HP-5MS capillary column (30 m, 0.25 mm, 0.25 μm phase thickness). The oven temperature program was as follows: 180°C for 1 min, 20°C/min to 250°C, 5°C/min to 300°C where the temperature was kept for 8 min, and then 35°C/min to 325°C. High purity helium was used as carrier gas at a flow rate of 0.8 mL/min in constant flow mode. The samples were injected in a splitless mode with an injection volume of 1 μL. The injector, transfer line and source temperatures were 270°C, 280°C and 250°C respectively. The mass spectrometer was operated in the selected ion monitoring (SIM) mode, and the following ions were monitored for analysis: 7α-hydroxycholesterol 456-367 m/z, 7β-hydroxycholesterol 456-367 m/z, 25-hydroxycholesterol 546-456 m/z, 7-ketocholesterol 472-382 m/z. Peak detection, integration and quantitative analysis were executed using Xcalibur Quantitative browser (ThermoScientific) based on calibration lines built with commercially available oxysterols standards (Avanti Polar Lipids or Interchim).

#### *2.14. GC-MS quantification of free cholesterol*

After treatments, total lipids were extracted from cell lysates according to the method of Bligh and Dyer [28] in chloroform/methanol/water (2:2:1.8; v/v), spiked with stigmaterol as internal standard, followed by sterols separation on TLC (hexane, diethyl ether, methanol, acetic acid, 50:50:5:1, v/v). Cholesterol was extracted from silica (hexane/diethyl ether, 1:1; v/v), dried under nitrogen and converted to its respective trimethylsilyl ether by treatment with BSTFA at room temperature, overnight. Gas chromatographic analysis was performed with a Hewlett Packard (HP-6890) and a J & W 122-4762 (60 m x 0.25 mm) capillary column. The eluted compounds were detected at the column outlet by a mass spectrometer (Hewlett Packard MS-5973) and quantified using the internal standard stigmaterol.

### **3. Results**

#### *3.1. Analysis of OSBP and ORPs mRNA expression in RAW264.7 macrophages*

First, we established the cellular response in RAW264.7 macrophages to native (nLDL) or oxidized LDL (oxLDL) loading, by determining the respective mRNA expression levels of OSBP/ORP. After exposure to nLDL the mRNA levels of OSBP, ORP1L, ORP8, ORP9 and ORP11 increased significantly compared to unloaded conditions (**Fig.1**). ORP2, ORP9 and most strikingly ORP11 mRNA levels were higher in oxLDL loaded macrophages. ORP11 has recently been described to be associated with both Golgi elements and endosomal compartments [24], indicating a putative role in the non-vesicular lipid transport between Golgi and endosomes. Furthermore, *OSBPL11* gene has been reported to be involved in cholesterol metabolism in obese patients [25] and facilitate cholesterol trafficking in skin fibroblasts [30]. Consequently, we focused our further efforts on ORP11, investigating its possible involvement in BMP mediated oxLDL-derived sterol regulation.

### *3.2. ORP11, a candidate implicated in BMP-mediated oxysterol traffic*

Next, we examined whether BMP accumulation would impact ORP11 expression in RAW264.7 macrophages. Consistent with the change in mRNA expression, ORP11 protein level was increased upon nLDL incubation and by almost two-fold upon oxLDL incubation (**Fig.2A**). In oxLDL BMP-enriched cells, ORP11 was further up-regulated, suggesting a functional relationship between BMP and ORP11. This prompted us to determine the endogenous subcellular distribution of ORP11 in RAW264.7 macrophages compared to BMP. Consistent with earlier reports in HEK293 and HuH7 cells (20), ORP11 strongly, but not exclusively, colocalized ( $M2=0.89\pm0.03$  vs.  $M1=0.67\pm0.04$ ) with GM130, a Golgi marker displaying a typical compact juxtannuclear distribution (**Fig.2B**). Additionally, ORP11 labelling also colocalized with BMP ( $M2=0.91\pm0.05$ ), known to be an endosomal resident in RAW264.7 macrophages and representing a typical punctated perinuclear pattern [17], consistent with a possible cooperation between these two factors involved in sterol trafficking.

### *3.3. Impact of ORP11 silencing on protective action of BMP towards oxLDL*

To further investigate the function of endogenous ORP11 protein in macrophages, we generated stably silenced RAW264.7 cells using shRNA lentiviruses targeting ORP11 mRNA, and ORP3 mRNA used as a non-relevant ORP protein. The gene silencing efficiency was determined by quantitative real-time RT-PCR after lentiviral transduction and selection. Cell pools transduced with each virus were independently selected two times and the silencing efficiencies were between 0 and 69%. shORP11.2 and shORP3.2 cell pools with the highest knock-down efficiency (69% and 70%, respectively) was chosen for further experiments and silencing efficiencies were determined at the protein level (**Fig.3A**). ORP11 and ORP3 knockdown efficiencies in these cell pools corresponded well to the level of mRNA reduction (Data not shown). ORP3 was chosen as a control for BMP enrichment, as well as cell viability, as it mediates cell adhesion, independently of cholesterol homeostasis [31,32]. Furthermore, ORP3 is localized in plasma membrane/ER Membrane Contact Sites (MCS) [12,33], but excluded from LE.

To fully validate our cell models, we ensured that BMP enrichment after PG supplementation was maintained after ORP11 and ORP3 silencing. As expected [26], incubation of control (shNT) RAW264.7 macrophages with PG lead to a 3-4 fold increase of cellular BMP in all tested conditions (**Fig.3B**). Importantly, BMP accumulation was maintained at similar levels in both ORP11 and ORP3 silenced cells (shORP11 and shORP3) compared to their respective controls. Furthermore, as shown in Table 1, BMP molecular species composition was similar between shNT11 and shOPR11 cells, as well as shNT3 and shORP3 cells.

In a previous report [5], we showed that oxLDL exposure induced cell death that was partially restored by BMP enrichment. These effects were not observed in both unloaded and nLDL loading conditions. Consistently, cell viability in both shNT11 and shNT3 cells was drastically affected after oxLDL exposure compared to nLDL-loaded cells (**Fig.4A**), and BMP enrichment reduced oxLDL negative effect as cell viability leapt from 2 % up to 20 %. By contrast, cell viability remained low at only 9% in BMP-enriched shORP11 cells, indicating that functional ORP11 is required for the protective effect of BMP. Importantly, this is specific to ORP11, as silencing of ORP3 had a different effect on the protective action of BMP against oxLDL-induced cytotoxicity. Contrariwise, the increase in cell viability upon BMP enrichment was higher in shORP3 cells compared to shNT3 cells.

Cytotoxicity of oxLDL has been shown to be at least partly mediated by C-7 proapoptotic oxysterols [6]. Consistently, oxLDL exposure was correlated to increased amounts of C-7 oxysterols (7 $\alpha$ -HC, 7 $\beta$ -HC and 7-keto) in both shNT11 and shORP11 cells (**Fig 4B**), as well as in shNT3 and shORP3 cells (**Fig 4C**). As expected, the production of oxysterol was very low in both control and nLDL conditions (**Fig 4B**). BMP accumulation significantly reduced C-7 oxysterols amounts in shNT11 and shNT3 cells. Importantly, silencing of ORP11 but not ORP3 suppressed this BMP effect. The content of enzymatically and non-enzymatically accessible 25-hydroxycholesterol (25-OH), which has greater or lesser cytotoxicity depending on the cell considered [4], was also increased upon oxLDL exposure in both shNT11 and ORP11 cells. No 25-OH was detected in shNT3 or shORP3 cells. In contrast to C-7 oxysterols, the production of 25-OH was unaffected by BMP enrichment (**Fig.4C**). Together these results demonstrate the dependency of functional ORP11, but not ORP3, in BMP protective effect against both oxLDL induced cell death and proapoptotic C-7 oxysterols formation. This suggests a functional interplay of ORP11 and BMP selectively affecting the proapoptotic production of oxysterols and a concerted action of ORP11 and BMP for sterol trafficking and metabolism in macrophages.

### *3.4. Impact of ORP11 silencing on the fate of oxLDL-derived cholesterol*

We further aimed to investigate the possible cooperation between BMP and ORP11 in regulating cholesterol homeostasis in RAW264.7 macrophages. Free cholesterol (FC) levels, were compared in shNT11 and shORP11 cells. As shown in (**Fig.5A**), in shNT11 cells, FC levels were similar in all tested conditions regardless nLDL/oxLDL exposure or BMP enrichment. ORP11 silencing did not change FC content in unloaded or nLDL-loaded cells, independently of BMP enrichment. In contrast, it induced FC accumulation upon oxLDL loading, which was further enhanced in BMP-enriched cells. These increases in cellular FC may be related to differences in cholesterol esterification or cholesterol efflux. Cholesterol esterification was measured as a proportion of radioactivity recovered in cholesterol ester (CE) after incubation with [<sup>3</sup>H]oleate for 24 h. Neither BMP enrichment nor ORP11 silencing modified the rate of cholesterol esterification markedly in oxLDL loaded cells (**Fig.5B**).

As macrophage cholesterol efflux is essentially dependent on the expression of ATP-binding cassette transporters ABCG1 and ABCA1 [34], we measured their mRNA expression in shORP11 cells by quantitative real-time RT-PCR. ABCG1 mRNA levels were significantly reduced in ORP11 silenced cells compared to control (**Fig.5C**) and further decreased under BMP-enrichment conditions. In contrast, no differences were observed in ABCA1 mRNA levels (**Fig.5D**). We then measured cholesterol efflux to HDL which is dependent of ABCG1 in macrophages whereas efflux to ApoA1 is only dependent of ABCA1 [35]. As expected from our previous report [5], BMP enrichment slightly but significantly reduced cholesterol efflux to HDL in oxLDL-loaded shNT11 cells (**Fig.6E**). Cholesterol efflux was reduced in shORP11 cells compared to shNT11 cells, and completely abolished in BMP-enriched shORP11 cells. This is in good agreement with the above observed reduction of ABCG1 expression upon ORP11 silencing. Even if it is difficult to compare changes in mRNA levels and % of efflux, these two parameters lead in the same direction. Together, these observations suggest that ORP11 is intrinsically and specifically involved in oxLDL-derived cholesterol retention/efflux and support a facilitating role of BMP in that process.

## **4. Discussion**

We previously demonstrated that BMP exerts a protective action against the pro-apoptotic effect of oxLDL on macrophages *via* a reduced production of intracellular pro-apoptotic oxysterols [5]. In the present study, we report a new role for ORP11 in modulating the protective action of BMP against oxLDL cytotoxic effects, putatively *via* the control of the intracellular trafficking of cholesterol/oxysterols. Our data suggest that in cultured macrophages BMP and ORP11 together control the sterol metabolism to dampen the generation of cytotoxic 7-oxysterols.

Human and mouse ORPs genes are expressed in a large variety of tissues [33,36–39], but there are clear differences in tissue-specific expression patterns between the members of the ORPs family [13,40,41]. In the present study, we confirmed the expression of eight OSBP/ORPs genes in mouse RAW264.7 macrophages and found that most ORP mRNAs are induced after exposure of the cells to nLDL, a major sterol carrier. More interestingly, three ORP genes were up-regulated upon incubation of the cells with oxLDL: ORP2, ORP9 and ORP11. ORP2 regulates the membrane contact between ER and lipid droplets, providing a plausible explanation for its up-regulation under oxLDL exposure [42–45]. ORP9 localizes at the Golgi/ER interface and regulates phosphatidylinositol-4-phosphate (PI4P) metabolism in Golgi membranes, competitively with ORP4S [46]. Recently, ORP11 was demonstrated to dimerize with ORP9 and to localize at the interface of Golgi complex and LE [24]. This is consistent with their concomitant upregulation upon oxLDL treatment, as oxLDL promotes endolysosomal lipid storage in macrophage foam cells [47].

Little is known about the functions of ORP11, but given its intracellular localization at the Golgi-LE interface [24], and that of BMP almost exclusively in LE [16,48], we envision that these two molecules could work together to egress oxLDL-derived cholesterol and/or oxysterols out of the endosomal compartment. Of interest, upregulation of ORP11 protein expression upon oxLDL exposure was enhanced in BMP enriched cells. Furthermore, a strong colocalization of BMP and ORP11 in the endosomal compartment was observed. To further analyze the function of ORP11, we generated stably silenced ORP11 depleted RAW264.7 macrophages. ORP3 silenced cells were chosen as non-relevant controls as ORP3 expression was not modulated by nLDL/oxLDL exposure in our cell model. Moreover, so far known functions of ORP3 are not related to sterol metabolism [31]. We observed as a key result that the protection of BMP against the cytotoxic effect of oxLDL was specifically impaired by ORP11 knock-down. Importantly, this could not be attributed to the lack of BMP or different BMP molecular species in shORP11/shORP3 cells since both amount and composition of BMP were similar to respective shNT cells. Impacts on cell death/survival have been reported for ORP8 [49,50], OSBP [51], ORP4 [52], and ORP9 [53], *via* protein–protein interactions or impacts on membrane lipid domains [7]. ORP11 affected cell viability significantly only after BMP accumulation, suggesting that this protein-phospholipid interaction is an essential link of the cell survival-promoting machinery, and that BMP needs ORP11 to protect cell viability. This hypothesis was supported by the oxysterol profile in ORP11 knock-down as the negative impact of ORP11 silencing on cell viability was correlated with an elevated level of pro-apoptotic 7-oxysterols. Cells overexpressing ORP11 displayed multilamellar bodies associated with the Golgi complex related to ORP11 intracellular localization at the LE-Golgi interface [24]. Moreover, ORP11 interacts with ORP9, a family member implicated in cholesterol transport between ER and Golgi membranes [54].

Vihervaara *et al.* [13] tested the effect of knocking down ORP1L, ORP3 or ORP8 in RAW264.7 macrophages, on the cellular lipidome. In basal conditions, levels of FC and CEs were elevated in ORP1L and ORP8 knock-down cells. Levels of PIs, PEs, or SMs were differently modified, revealing distinct roles of the different ORPs as regulators of macrophage lipid composition. In the present work we showed that both ORP11 and ORP3

silencing did not interfere with BMP metabolism, as similar amounts of BMP were observed compared to shNT controls. The fact that BMP molecular species were not changed may suggest that ORP11 and ORP3 do not impact either on fatty acid metabolism. By contrast, ORP11 silencing increased the cellular cholesterol content in the presence of oxLDL, the effect being amplified after BMP accumulation, indicating a cumulative effect of ORP11 and BMP to regulate LE cholesterol levels. The increase of free cholesterol in ORP11 knock-down cells was not associated with a reduction of cholesterol esterification, indicating that ORP11 is not required for cholesterol transport from LE to the ER. However, cholesterol efflux to HDL was markedly reduced in ORP11 silenced cells after BMP accumulation, concomitant with reduced *ABCG1* expression. Related functions have been assigned for several ORP family members: Knock-down of ORP8 up-regulated cholesterol biosynthesis in hepatic cells through sterol regulatory element binding protein (SREBP) activity [55] and induced FC accumulation in macrophages [13] apparently *via* the inhibition of its efflux through ABCA1 [41]. ORP1L deficient macrophage displayed an increase of FC and CE, due to the inhibition of cholesterol efflux [56], and it was proposed that ORP1L impacts the endosomal cholesterol transport *via* the formation of MCSs between LE and ER [57–59]. ORP5 was suggested to mediate cholesterol egress from the LE limiting membrane in concert with Niemann-Pick C1 [60]; however, ORP5 and ORP8 were also identified as dual PS/PI4P transporters [61,62]. The closely related ORP2 has the capacity to enhance the transport of newly synthesized cholesterol to the cell surface [63] and during steroid hormone biosynthesis *via* LXR [64]. Moreover, OSBP negatively regulates ABCA1 protein stability and consequently the cellular cholesterol efflux capacity [65].

OSBP/ORPs proteins have been originally characterized as sterol sensors and/or transporters at membrane contact sites (MCS) between ER and other organelles [11,12]. More recently, this role was expanded to the binding /transfer of glycerophospholipids [66], such as PI4P [10,61,67–70], phosphatidylinositol bisphosphate (PIP<sub>2</sub>) [62,71] or Phosphatidylserine (PS) [69,72,73]. Similarly, ORP11 localizes *via* its N-terminal domain in Golgi and LE membranes, and is implicated in non-vesicular communication between these two organelles [24]. We propose that, in cooperation with BMP, ORP11 could act as a key component of a new pathway of non-vesicular lipid transport between LE and Golgi. BMP could be considered as a potential ligand of the ORD on ORP11, which could act as lipid signal to stimulate the egress of cholesterol from LE. This non-vesicular transport could be facilitated by a MCS between these two organelles [11,74]. ORP11 could act directly as a cholesterol carrier stimulated by BMP or *via* a yet known partner like NPC2 regulation as described for NPC1 [75–77]. However, Maeda *et al.* [72] classified ORP11 within a clade that may not bind/transport cholesterol. Therefore, we find it possible that ORP11 may promote sterol transport indirectly *via* regulation of the assembly or function of a MCS. Further study of a putative molecular interaction between BMP and ORP11 by employing biomimetic membranes and liposomes will be crucial for elucidating the mechanism of ORP11 action and its modulation by BMP.

To conclude, the present work identifies ORP11 as a regulator of macrophage cholesterol homeostasis. ORP11 regulates the cytotoxicity of oxLDL and oxysterols *via* the endosomal phospholipid, BMP, as well as cholesterol efflux from macrophages. Consistent with the genetic findings of Bouchard *et al.* [25], ORP11 may thus act as a modulator of atherosclerosis.

### Funding

This study was supported by grants from INSA-Lyon, INSERM, from the Avenir Lyon Saint-Etienne program and Rhône-Alpes region, from the Academy of Finland (285223), the Sigrid

Juselius Foundation, and the Magnus Ehrnrooth Foundation (V.M.O). GC-MS analyses were performed on the Toulouse INSERM Metatoul-Lipidomique Core Facility-MetaboHub ANR-11-INBS-010

### **Acknowledgments**

We gratefully acknowledge Riikka Kosonen for skilled technical assistance.

**Conflict of interest:** The authors declare that they have no conflicts of interest with the contents of this article.

**Author contributions:** M.A.L. helped design the experiments, generated molecular tools, and acquired the vast majority of the data. She also analyzed and interpreted the data as well as drafted the article. Y.C. performed cholesterol quantification and efflux experiments. P.G. performed LC-MS analysis of BMP. K.G. and F.C. performed qRT-PCR analysis. F.R. and J.B.M. performed GC-MS analysis of oxysterols. F.H.M. helped in critical revision of the manuscript. V.M.O. designed ORPs screening and molecular biological study. I.D. and C.L.C. designed the study and wrote the paper. All authors reviewed and approved the final version of the manuscript.

### **References**

- [1] N. Shibata, C.K. Glass, Macrophages, oxysterols and atherosclerosis, *Circ. J.* 74 (2010) 2045–2051.
- [2] Y. Chen, M. Arnal-Levron, M. Lagarde, P. Moulin, C. Luquain-Costaz, I. Delton, THP1 macrophages oxidized cholesterol, generating 7-derivative oxysterols specifically released by HDL, *Steroids.* 99 (2015) 212–8. doi:10.1016/j.steroids.2015.02.020.
- [3] D.A. Larsson, S. Baird, J.D. Nyhalah, X.M. Yuan, W. Li, Oxysterol mixtures, in atheroma-relevant proportions, display synergistic and proapoptotic effects, *Free Radic Biol Med.* 41 (2006) 902–10. doi:10.1016/j.freeradbiomed.2006.05.032.
- [4] A. Vejux, G. Lizard, Cytotoxic effects of oxysterols associated with human diseases: Induction of cell death (apoptosis and/or oncosis), oxidative and inflammatory activities, and phospholipidosis, *Mol Aspects Med.* 30 (2009) 153–70. doi:10.1016/j.mam.2009.02.006.
- [5] M. Arnal-Levron, Y. Chen, I. Delton-Vandenbroucke, C. Luquain-Costaz, Bis(monoacylglycero)phosphate reduces oxysterol formation and apoptosis in macrophages exposed to oxidized LDL, *Biochem. Pharmacol.* 86 (2013) 115–121. doi:10.1016/j.bcp.2013.03.017.
- [6] A. Nègre-Salvayre, N. Augé, C. Camaré, T. Bacchetti, G. Ferretti, R. Salvayre, Dual signaling evoked by oxidized LDLs in vascular cells, *Free Radic. Biol. Med.* 106 (2017) 118–133. doi:10.1016/j.freeradbiomed.2017.02.006.
- [7] V.M. Olkkonen, Macrophage oxysterols and their binding proteins: roles in atherosclerosis, *Curr Opin Lipidol.* 23 (2012) 462–70. doi:10.1097/MOL.0b013e328356dba0.
- [8] V.M. Olkkonen, O. Beaslas, E. Nissila, Oxysterols and their cellular effectors, *Biomolecules.* 2 (2012) 76–103. doi:10.3390/biom2010076.
- [9] D.E. Dye, M.A. Bieniawski, S.C.E. Wright, A. McCauley, D.R. Coombe, C.J. Mousley, The Fundamental And Pathological Importance Of Oxysterol Binding Protein And Its Related Proteins, *J. Lipid Res.* (2018). doi:10.1194/jlr.R088682.
- [10] A. Pietrangelo, N.D. Ridgway, Bridging the molecular and biological functions of the oxysterol-binding protein family, *Cell. Mol. Life Sci.* (2018). doi:10.1007/s00018-018-2795-y.

- [11] H. Kentala, M. Weber-Boyvatt, V.M. Olkkonen, OSBP-Related Protein Family: Mediators of Lipid Transport and Signaling at Membrane Contact Sites, *Int Rev Cell Mol Biol.* 321 (2016) 299–340. doi:10.1016/bs.ircmb.2015.09.006.
- [12] V.M. Olkkonen, S. Li, Oxysterol-binding proteins: sterol and phosphoinositide sensors coordinating transport, signaling and metabolism, *Prog Lipid Res.* 52 (2013) 529–38. doi:10.1016/j.plipres.2013.06.004.
- [13] T. Vihervaara, R. Kakela, G. Liebisch, K. Tarasov, G. Schmitz, V.M. Olkkonen, Modification of the lipidome in RAW264.7 macrophage subjected to stable silencing of oxysterol-binding proteins, *Biochimie.* 95 (2013) 538–47. doi:10.1016/j.biochi.2012.05.004.
- [14] I. Delton-Vandenbroucke, J. Bouvier, A. Makino, N. Besson, J.F. Pageaux, M. Lagarde, T. Kobayashi, Anti-bis(monoacylglycero)phosphate antibody accumulates acetylated LDL-derived cholesterol in cultured macrophages, *J Lipid Res.* 48 (2007) 543–52. doi:10.1194/jlr.M600266-JLR200.
- [15] J. Chevallier, Z. Chamoun, G. Jiang, G. Prestwich, N. Sakai, S. Matile, R.G. Parton, J. Gruenberg, Lysobisphosphatidic acid controls endosomal cholesterol levels, *J Biol Chem.* 283 (2008) 27871–80. doi:10.1074/jbc.M801463200.
- [16] T. Kobayashi, M.H. Beuchat, M. Lindsay, S. Frias, R.D. Palmiter, H. Sakuraba, R.G. Parton, J. Gruenberg, Late endosomal membranes rich in lysobisphosphatidic acid regulate cholesterol transport, *Nat Cell Biol.* 1 (1999) 113–8. doi:10.1038/10084.
- [17] C. Luquain-Costaz, E. Lefai, M. Arnal-Levron, D. Markina, S. Sakai, V. Euthine, A. Makino, M. Guichardant, S. Yamashita, T. Kobayashi, M. Lagarde, P. Moulin, I. Delton-Vandenbroucke, Bis(monoacylglycero)phosphate accumulation in macrophages induces intracellular cholesterol redistribution, attenuates liver-X receptor/ATP-Binding cassette transporter A1/ATP-binding cassette transporter G1 pathway, and impairs cholesterol efflux, *Arterioscler Thromb Vasc Biol.* 33 (2013) 1803–11. doi:10.1161/ATVBAHA.113.301857.
- [18] M.T. Vanier, Complex lipid trafficking in Niemann-Pick disease type C, *J Inherit Metab Dis.* 38 (2015) 187–99. doi:10.1007/s10545-014-9794-4.
- [19] J.R. Zhang, T. Coleman, S.J. Langmade, D.E. Scherrer, L. Lane, M.H. Lanier, C. Feng, M.S. Sands, J.E. Schaffer, C.F. Semenkovich, D.S. Ory, Niemann-Pick C1 protects against atherosclerosis in mice via regulation of macrophage intracellular cholesterol trafficking, *J Clin Invest.* 118 (2008) 2281–90. doi:10.1172/JCI32561.
- [20] M.C. Vazquez, E. Balboa, A.R. Alvarez, S. Zanlungo, Oxidative stress: a pathogenic mechanism for Niemann-Pick type C disease, *Oxid Med Cell Longev.* 2012 (2012) 205713. doi:10.1155/2012/205713.
- [21] M. Abdul-Hammed, B. Breiden, M.A. Adebayo, J.O. Babalola, G. Schwarzmann, K. Sandhoff, Role of endosomal membrane lipids and NPC2 in cholesterol transfer and membrane fusion, *J Lipid Res.* 51 (2010) 1747–60. doi:10.1194/jlr.M003822.
- [22] Z. Xu, W. Farver, S. Kodukula, J. Storch, Regulation of sterol transport between membranes and NPC2, *Biochemistry.* 47 (2008) 11134–43. doi:10.1021/bi801328u.
- [23] H.D. Gallala, K. Sandhoff, Biological function of the cellular lipid BMP-BMP as a key activator for cholesterol sorting and membrane digestion, *Neurochem Res.* 36 (2011) 1594–600. doi:10.1007/s11064-010-0337-6.
- [24] Y. Zhou, S. Li, M.I. Mayranpaa, W. Zhong, N. Back, D. Yan, V.M. Olkkonen, OSBP-related protein 11 (ORP11) dimerizes with ORP9 and localizes at the Golgi-late endosome interface, *Exp Cell Res.* 316 (2010) 3304–16. doi:10.1016/j.yexcr.2010.06.008.
- [25] L. Bouchard, G. Faucher, A. Tchernof, Y. Deshaies, S. Marceau, O. Lescelleur, S. Biron, C. Bouchard, L. Perusse, M.C. Vohl, Association of OSBPL11 gene polymorphisms with cardiovascular disease risk factors in obesity, *Obesity (Silver Spring).* 17 (2009) 1466–72. doi:10.1038/oby.2009.71.
- [26] J. Bouvier, K.A. Zemski Berry, F. Hullin-Matsuda, A. Makino, S. Michaud, A. Geloën, R.C. Murphy, T. Kobayashi, M. Lagarde, I. Delton-Vandenbroucke, Selective decrease of

- bis(monoacylglycero)phosphate content in macrophages by high supplementation with docosahexaenoic acid, *J Lipid Res.* 50 (2009) 243–55. doi:10.1194/jlr.M800300-JLR200.
- [27] R.J. Havel, H.A. Eder, J.H. Bragdon, The distribution and chemical composition of ultracentrifugally separated lipoproteins in human serum, *J Clin Invest.* 34 (1955) 1345–53. doi:10.1172/JCI103182.
- [28] E.G. Bligh, W.J. Dyer, A rapid method of total lipid extraction and purification, *Can J Biochem Physiol.* 37 (1959) 911–917. doi:10.1139/o59-099.
- [29] L. Iuliano, F. Micheletta, S. Natoli, S. Ginanni Corradini, M. Iappelli, W. Elisei, L. Giovannelli, F. Violi, U. Diczfalusy, Measurement of oxysterols and alpha-tocopherol in plasma and tissue samples as indices of oxidant stress status, *Anal Biochem.* 312 (2003) 217–23.
- [30] B. Kara, Ç. Köroğlu, K. Peltonen, R.C. Steinberg, H. Maraş Genç, M. Hölttä-Vuori, A. Güven, K. Kanerva, T. Kotil, S. Solakoğlu, Y. Zhou, V.M. Olkkonen, E. Ikonen, M. Laiho, A. Tolun, Severe neurodegenerative disease in brothers with homozygous mutation in POLR1A, *Eur J Hum Genet.* 25 (2017) 315–323. doi:10.1038/ejhg.2016.183.
- [31] M. Weber-Boyyat, H. Kentala, J. Lilja, T. Vihervaara, R. Hanninen, Y. Zhou, J. Peränen, T.A. Nyman, J. Ivaska, V.M. Olkkonen, OSBP-related protein 3 (ORP3) coupling with VAMP-associated protein A regulates R-Ras activity, *Exp. Cell Res.* 331 (2015) 278–291. doi:10.1016/j.yexcr.2014.10.019.
- [32] M. Lehto, M.I. Mäyränpää, T. Pellinen, P. Ihalmo, S. Lehtonen, P.T. Kovanen, P.-H. Groop, J. Ivaska, V.M. Olkkonen, The R-Ras interaction partner ORP3 regulates cell adhesion, *J. Cell. Sci.* 121 (2008) 695–705. doi:10.1242/jcs.016964.
- [33] M. Lehto, J. Tienari, S. Lehtonen, E. Lehtonen, V.M. Olkkonen, Subfamily III of mammalian oxysterol-binding protein (OSBP) homologues: the expression and intracellular localization of ORP3, ORP6, and ORP7, *Cell Tissue Res.* 315 (2004) 39–57. doi:10.1007/s00441-003-0817-y.
- [34] L. Yvan-Charvet, N. Wang, A.R. Tall, Role of HDL, ABCA1, and ABCG1 transporters in cholesterol efflux and immune responses, *Arterioscler Thromb Vasc Biol.* 30 (2010) 139–43. doi:10.1161/ATVBAHA.108.179283.
- [35] M.C. Phillips, Molecular mechanisms of cellular cholesterol efflux, *J. Biol. Chem.* 289 (2014) 24020–24029. doi:10.1074/jbc.R114.583658.
- [36] S. Laitinen, V.M. Olkkonen, C. Ehnholm, E. Ikonen, Family of human oxysterol binding protein (OSBP) homologues. A novel member implicated in brain sterol metabolism, *J Lipid Res.* 40 (1999) 2204–11.
- [37] M. Lehto, S. Laitinen, G. Chinetti, M. Johansson, C. Ehnholm, B. Staels, E. Ikonen, V.M. Olkkonen, The OSBP-related protein family in humans, *J Lipid Res.* 42 (2001) 1203–13.
- [38] C.J. Jaworski, E. Moreira, A. Li, R. Lee, I.R. Rodriguez, A family of 12 human genes containing oxysterol-binding domains, *Genomics.* 78 (2001) 185–96. doi:10.1006/geno.2001.6663.
- [39] A.M. Anniss, J. Apostolopoulos, S. Dworkin, L.E. Purton, R.L. Sparrow, An oxysterol-binding protein family identified in the mouse, *DNA Cell Biol.* 21 (2002) 571–80. doi:10.1089/104454902320308942.
- [40] D. Yan, M. Jauhiainen, R.B. Hildebrand, K. Willems van Dijk, T.J. Van Berkel, C. Ehnholm, M. Van Eck, V.M. Olkkonen, Expression of human OSBP-related protein 1L in macrophages enhances atherosclerotic lesion development in LDL receptor-deficient mice, *Arterioscler Thromb Vasc Biol.* 27 (2007) 1618–24. doi:10.1161/ATVBAHA.107.144121.
- [41] D. Yan, M.I. Mayranpaa, J. Wong, J. Perttila, M. Lehto, M. Jauhiainen, P.T. Kovanen, C. Ehnholm, A.J. Brown, V.M. Olkkonen, OSBP-related protein 8 (ORP8) suppresses ABCA1 expression and cholesterol efflux from macrophages, *J Biol Chem.* 283 (2008) 332–40. doi:10.1074/jbc.M705313200.
- [42] E. Orso, M. Grandl, G. Schmitz, Oxidized LDL-induced endolysosomal phospholipidosis and enzymatically modified LDL-induced foam cell formation determine specific lipid species modulation in human macrophages, *Chem Phys Lipids.* 164 (2011) 479–87. doi:10.1016/j.chemphyslip.2011.06.001.

- [43] H. Kentala, S.G. Pfisterer, V.M. Olkkonen, M. Weber-Boyvat, Sterol liganding of OSBP-related proteins (ORPs) regulates the subcellular distribution of ORP-VAPA complexes and their impacts on organelle structure, *Steroids*. 99 (2015) 248–58. doi:10.1016/j.steroids.2015.01.027.
- [44] M. Weber-Boyvat, H. Kentala, J. Peranen, V.M. Olkkonen, Ligand-dependent localization and function of ORP-VAP complexes at membrane contact sites, *Cell Mol Life Sci*. 72 (2015) 1967–87. doi:10.1007/s00018-014-1786-x.
- [45] H. Kentala, A. Koponen, H. Vihinen, J. Pirhonen, G. Liebisch, Z. Pataj, A. Kivelä, S. Li, L. Karhinen, E. Jääskeläinen, R. Andrews, L. Meriläinen, S. Matysik, E. Ikonen, Y. Zhou, E. Jokitalo, V.M. Olkkonen, OSBP-related protein-2 (ORP2): a novel Akt effector that controls cellular energy metabolism, *Cell. Mol. Life Sci.* (2018). doi:10.1007/s00018-018-2850-8.
- [46] X. Liu, N.D. Ridgway, Characterization of the sterol and phosphatidylinositol 4-phosphate binding properties of Golgi-associated OSBP-related protein 9 (ORP9), *PLoS One*. 9 (2014) e108368. doi:10.1371/journal.pone.0108368.
- [47] G. Schmitz, M. Grandl, Endolysosomal phospholipidosis and cytosolic lipid droplet storage and release in macrophages, *Biochim Biophys Acta*. 1791 (2009) 524–39. doi:10.1016/j.bbali.2008.12.007.
- [48] F. Hullin-Matsuda, C. Luquain-Costaz, J. Bouvier, I. Delton-Vandenbroucke, Bis(monoacylglycero)phosphate, a peculiar phospholipid to control the fate of cholesterol: Implications in pathology, *Prostaglandins Leukot Essent Fatty Acids*. 81 (2009) 313–24. doi:10.1016/j.plefa.2009.09.006.
- [49] W. Zhong, S. Qin, B. Zhu, M. Pu, F. Liu, L. Wang, G. Ye, Q. Yi, D. Yan, Oxysterol-binding protein-related protein 8 (ORP8) increases sensitivity of hepatocellular carcinoma cells to Fas-mediated apoptosis, *J Biol Chem*. 290 (2015) 8876–87. doi:10.1074/jbc.M114.610188.
- [50] J. Li, X. Zheng, N. Lou, W. Zhong, D. Yan, Oxysterol binding protein-related protein 8 mediates the cytotoxicity of 25-hydroxycholesterol, *J. Lipid Res*. 57 (2016) 1845–1853. doi:10.1194/jlr.M069906.
- [51] A.W. Burgett, T.B. Poulsen, K. Wangkanont, D.R. Anderson, C. Kikuchi, K. Shimada, S. Okubo, K.C. Fortner, Y. Mimaki, M. Kuroda, J.P. Murphy, D.J. Schwalb, E.C. Petrella, I. Cornella-Taracido, M. Schirle, J.A. Tallarico, M.D. Shair, Natural products reveal cancer cell dependence on oxysterol-binding proteins, *Nat Chem Biol*. 7 (2011) 639–47. doi:10.1038/nchembio.625.
- [52] M. Charman, T.R. Colbourne, A. Pietrangelo, L. Kreplak, N.D. Ridgway, Oxysterol-binding protein (OSBP)-related protein 4 (ORP4) is essential for cell proliferation and survival, *J Biol Chem*. 289 (2014) 15705–17. doi:10.1074/jbc.M114.571216.
- [53] E. Lessmann, M. Ngo, M. Leitges, S. Minguet, N.D. Ridgway, M. Huber, Oxysterol-binding protein-related protein (ORP) 9 is a PDK-2 substrate and regulates Akt phosphorylation, *Cell Signal*. 19 (2007) 384–92. doi:10.1016/j.cellsig.2006.07.009.
- [54] M. Ngo, N.D. Ridgway, Oxysterol binding protein-related Protein 9 (ORP9) is a cholesterol transfer protein that regulates Golgi structure and function, *Mol Biol Cell*. 20 (2009) 1388–99. doi:10.1091/mbc.E08-09-0905.
- [55] T. Zhou, S. Li, W. Zhong, T. Vihervaara, O. Beaslas, J. Perttila, W. Luo, Y. Jiang, M. Lehto, V.M. Olkkonen, D. Yan, OSBP-related protein 8 (ORP8) regulates plasma and liver tissue lipid levels and interacts with the nucleoporin Nup62, *PLoS One*. 6 (2011) e21078. doi:10.1371/journal.pone.0021078.
- [56] T. Vihervaara, R.L. Uronen, G. Wohlfahrt, I. Bjorkhem, E. Ikonen, V.M. Olkkonen, Sterol binding by OSBP-related protein 1L regulates late endosome motility and function, *Cell Mol Life Sci*. 68 (2011) 537–51. doi:10.1007/s00018-010-0470-z.
- [57] N. Rocha, C. Kuijl, R. van der Kant, L. Janssen, D. Houben, H. Janssen, W. Zwart, J. Neefjes, Cholesterol sensor ORP1L contacts the ER protein VAP to control Rab7-RILP-p150 Glued and late endosome positioning, *J Cell Biol*. 185 (2009) 1209–25. doi:10.1083/jcb.200811005.
- [58] A.A. Rowland, P.J. Chitwood, M.J. Phillips, G.K. Voeltz, ER contact sites define the position and timing of endosome fission, *Cell*. 159 (2014) 1027–41. doi:10.1016/j.cell.2014.10.023.

- [59] K. Zhao, N.D. Ridgway, Oxysterol-Binding Protein-Related Protein 1L Regulates Cholesterol Egress from the Endo-Lysosomal System, *Cell Rep.* 19 (2017) 1807–1818. doi:10.1016/j.celrep.2017.05.028.
- [60] X. Du, J. Kumar, C. Ferguson, T.A. Schulz, Y.S. Ong, W. Hong, W.A. Prinz, R.G. Parton, A.J. Brown, H. Yang, A role for oxysterol-binding protein-related protein 5 in endosomal cholesterol trafficking, *J Cell Biol.* 192 (2011) 121–35. doi:10.1083/jcb.201004142.
- [61] J. Chung, F. Torta, K. Masai, L. Lucast, H. Czaplá, L.B. Tanner, P. Narayanaswamy, M.R. Wenk, F. Nakatsu, P. De Camilli, INTRACELLULAR TRANSPORT. PI4P/phosphatidylserine countertransport at ORP5- and ORP8-mediated ER-plasma membrane contacts, *Science.* 349 (2015) 428–32. doi:10.1126/science.aab1370.
- [62] R. Ghai, X. Du, H. Wang, J. Dong, C. Ferguson, A.J. Brown, R.G. Parton, J.-W. Wu, H. Yang, ORP5 and ORP8 bind phosphatidylinositol-4, 5-biphosphate (PtdIns(4,5)P<sub>2</sub>) and regulate its level at the plasma membrane, *Nat Commun.* 8 (2017) 757. doi:10.1038/s41467-017-00861-5.
- [63] R. Hynynen, S. Laitinen, R. Kakela, K. Tanhuanpaa, S. Lusa, C. Ehnholm, P. Somerharju, E. Ikonen, V.M. Olkkonen, Overexpression of OSBP-related protein 2 (ORP2) induces changes in cellular cholesterol metabolism and enhances endocytosis, *Biochem J.* 390 (2005) 273–83. doi:10.1042/BJ20042082.
- [64] T. Escajadillo, H. Wang, L. Li, D. Li, M.B. Sewer, Oxysterol-related-binding-protein related Protein-2 (ORP2) regulates cortisol biosynthesis and cholesterol homeostasis, *Mol. Cell. Endocrinol.* 427 (2016) 73–85. doi:10.1016/j.mce.2016.03.006.
- [65] K. Bowden, N.D. Ridgway, OSBP negatively regulates ABCA1 protein stability, *J Biol Chem.* 283 (2008) 18210–7. doi:10.1074/jbc.M800918200.
- [66] V.M. Olkkonen, OSBP-related proteins: liganding by glycerophospholipids opens new insight into their function, *Molecules.* 18 (2013) 13666–79. doi:10.3390/molecules181113666.
- [67] M. de Saint-Jean, V. Delfosse, D. Douguet, G. Chicanne, B. Payrastre, W. Bourguet, B. Antonny, G. Drin, Osh4p exchanges sterols for phosphatidylinositol 4-phosphate between lipid bilayers, *J Cell Biol.* 195 (2011) 965–78. doi:10.1083/jcb.201104062.
- [68] B. Mesmin, J. Bigay, J. Moser von Filseck, S. Lacas-Gervais, G. Drin, B. Antonny, A four-step cycle driven by PI(4)P hydrolysis directs sterol/PI(4)P exchange by the ER-Golgi tether OSBP, *Cell.* 155 (2013) 830–43. doi:10.1016/j.cell.2013.09.056.
- [69] J. Moser von Filseck, A. Copic, V. Delfosse, S. Vanni, C.L. Jackson, W. Bourguet, G. Drin, INTRACELLULAR TRANSPORT. Phosphatidylserine transport by ORP/Osh proteins is driven by phosphatidylinositol 4-phosphate, *Science.* 349 (2015) 432–6. doi:10.1126/science.aab1346.
- [70] B. Antonny, J. Bigay, B. Mesmin, The Oxysterol-Binding Protein Cycle: Burning Off PI(4)P to Transport Cholesterol, *Annu. Rev. Biochem.* 87 (2018) 809–837. doi:10.1146/annurev-biochem-061516-044924.
- [71] S. Raychaudhuri, Y.J. Im, J.H. Hurley, W.A. Prinz, Nonvesicular sterol movement from plasma membrane to ER requires oxysterol-binding protein-related proteins and phosphoinositides, *J Cell Biol.* 173 (2006) 107–19. doi:10.1083/jcb.200510084.
- [72] K. Maeda, K. Anand, A. Chiapparino, A. Kumar, M. Poletto, M. Kaksonen, A.C. Gavin, Interactome map uncovers phosphatidylserine transport by oxysterol-binding proteins, *Nature.* 501 (2013) 257–61. doi:10.1038/nature12430.
- [73] R. Iwama, M. Hara, A. Mizuike, H. Horiuchi, R. Fukuda, Osh6p, a homologue of the oxysterol-binding protein, is involved in production of functional cytochrome P450 belonging to CYP52 family in n-alkane-assimilating yeast *Yarrowia lipolytica*, *Biochem. Biophys. Res. Commun.* 499 (2018) 836–842. doi:10.1016/j.bbrc.2018.04.002.
- [74] W.A. Prinz, Bridging the gap: membrane contact sites in signaling, metabolism, and organelle dynamics, *J Cell Biol.* 205 (2014) 759–69. doi:10.1083/jcb.201401126.
- [75] J. Storch, Z. Xu, Niemann-Pick C2 (NPC2) and intracellular cholesterol trafficking, *Biochim Biophys Acta.* 1791 (2009) 671–8. doi:10.1016/j.bbali.2009.02.001.

- [76] L.A. McCauliff, Z. Xu, R. Li, S. Kodukula, D.C. Ko, M.P. Scott, P.C. Kahn, J. Storch, Multiple Surface Regions on the Niemann-Pick C2 Protein Facilitate Intracellular Cholesterol Transport, *J Biol Chem.* 290 (2015) 27321–31. doi:10.1074/jbc.M115.667469.
- [77] J. Luo, L. Jiang, H. Yang, B.-L. Song, Routes and mechanisms of post-endosomal cholesterol trafficking: A story that never ends, *Traffic.* 18 (2017) 209–217. doi:10.1111/tra.12471.

## Figures legends

**Fig.1. Expression level of major OSBP/ORP mRNA in RAW264.7 macrophages.** Cells were incubated in the absence or presence of 100µg/ml nLDL or 200µg/ml oxLDL for 24h. Cells were analyzed for different mRNA content by qPCR. Data are means±SD of 3 wells and are representative of 2 independent experiments. a,  $p < 0,05$  compared to unloaded; b,  $p < 0,05$  compared to nLDL

**Fig.2. ORP11 expression in RAW macrophages.** (A) Western Blotting analysis of endogenous ORP11 protein. Control and BMP-enriched cells were incubated in the presence of 100µg/ml nLDL or 200µg/ml oxLDL for 24h (upper panel). Quantification of ORP11 protein was related to tubulin. Data are mean±SD of 3 wells and are representative of 2 independent experiments. a,  $p < 0,05$  compared to control; b,  $p < 0,05$  compared to nLDL; c,  $p < 0,05$  compared to oxLDL (lower panel). (B) Intracellular localization of endogenous ORP11 by confocal microscopy double staining with anti-ORP11 (red) and anti GM130 (green) or anti-BMP (green) antibodies. Colocalization scores using Manders' overlap coefficient (M1 and M2) were calculated for individual cells representative of the population of cells (minimum of 15 cells per conditions) using Just Another Colocalization Plugin (JACoP) for ImageJ. M1 represents the fraction of the red signal overlapping the green signal and M2 represents the fraction of the green signal overlapping the red signal.

**Fig.3. Characterization of RAW264.7 macrophages subjected to ORP11 knock-down.** (A) A representative Western Blotting of RAW macrophages showing efficiency of silencing for ORP11 (90%) and ORP3 (85%) at the protein level ORP11 (shORP11.2) and ORP3 (shORP3.2) (B) Effect of ORP11 silencing on BMP level. Unloaded and BMP-enriched shNT, shORP11, shNT3 or shORP3 cells where incubated with 100µg/ml nLDL or 200µg/ml oxLDL for 24h. BMP was quantified by liquid chromatography-mass spectrometry as described in M&M. Data are the means±SD of 3 wells and representative of 3 independent experiments. a,  $p < 0,05$  compared to control; b,  $p < 0,05$  compared to nLDL; c,  $p < 0,05$  compared to oxLDL; d,  $p < 0,05$  compared to oxLDL BMP enriched in shNT cells.

**Fig.4. Effect of ORP11 silencing on protective action of BMP towards oxLDL.** Control and BMP-enriched shNT, shORP11 or shOPR3 cells where incubated with 100µg/ml nLDL or 200µg/ml oxLDL for 24h. (A) Cell viability was evaluated. Data are the means±SD of 3 wells and representative of 3 independent experiments. a,  $p < 0,05$  compared to nLDL; b,  $p < 0,05$  compared to oxLDL; c,  $p < 0,05$  compared to shNT oxLDL BMP enriched cells; d,  $p < 0,05$  compared to shNT3 oxLDL BMP enriched. Control and BMP-enriched shNT or shORP11 cells where incubated in the absence or presence of 100µg/ml nLDL or 200µg/ml oxLDL for 24h. (B and C) 7-oxycholesterols (7α-, 7β-hydroxycholesterol, and 7-ketocholesterol) and 25-hydroxycholesterols (D) were quantified by GC-MS/MS as described in M&M. Data are the means±SD of 3 wells and representative of 3 independent experiments. a,  $p < 0,05$  compared oxLDL, b,  $p < 0,05$  compared to shNT oxLDL BMP enriched.

**Fig.5. Effect of ORP11 silencing on cellular cholesterol fate.** Unloaded and BMP-enriched shNT or shORP11 cells where incubated in the absence or presence of 100µg/ml nLDL or 200µg/ml oxLDL for 24h. (A) Free cholesterol (FC) was quantified by GC/MS as described in M&M. Data are the means±SD of 3 wells and representative of 2 independent experiments. a,  $p < 0,05$  compared to shNT oxLDL cells; b,  $p < 0,05$  compared to shNT oxLDL BMP enriched; c,  $p < 0,05$  compared to shORP11 oxLDL. (B) Cells where incubated with [<sup>3</sup>H] oleate and cholesterol esterification was measured as the proportion of radioactivity recovered in CE. ABCG1 (C) and ABCA1 (D) mRNA content was measured by RT-PCR as described in M&M. a,  $p < 0,05$  compared to shNT oxLDL; b,  $p < 0,05$  compared to shNT oxLDL BMP enriched; c,  $p < 0,05$  compared to shORP11 oxLDL. (E) Cells where incubated with [<sup>3</sup>H] cholesterol for 24h. Cholesterol efflux was stimulated by 100µg/ml HDL for 6 hours. Data are the means±SD of 3 wells and representative of 3 independent experiments. a,  $p < 0,05$  compared to shNT oxLDL; b,  $p < 0,05$  compared to shNT oxLDL; c,  $p < 0,05$  compared to shNT oxLDL BMP enriched; d,  $p < 0,05$  compared to shORP11 oxLDL.

Figure 1

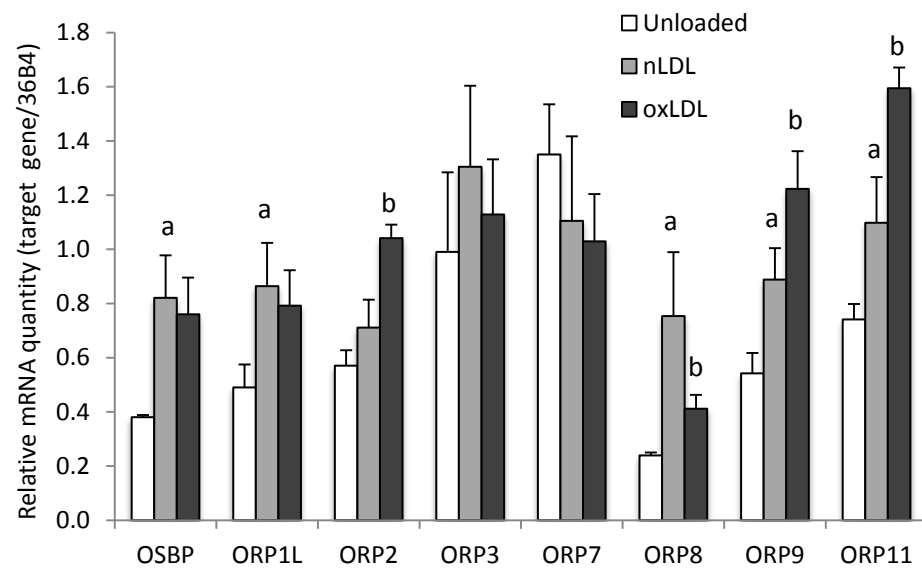
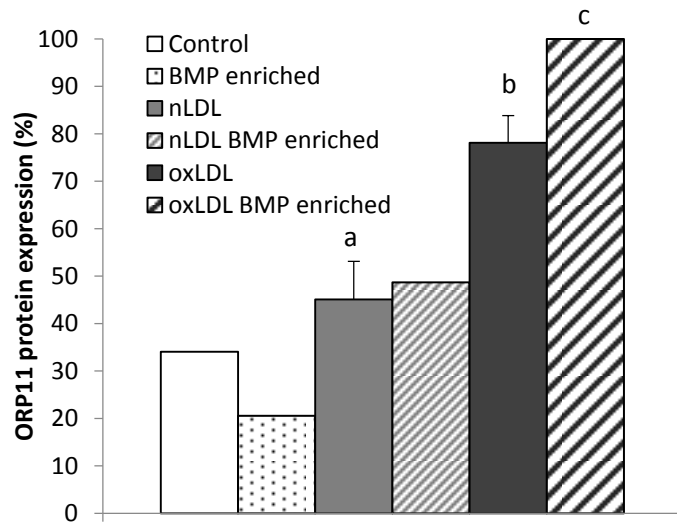
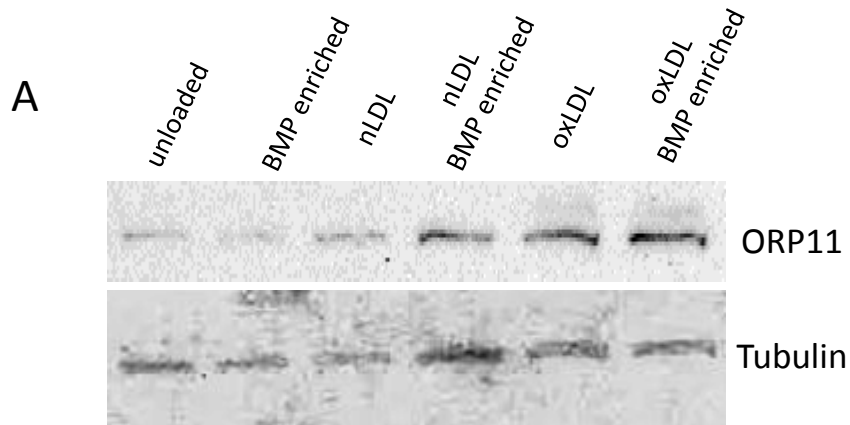
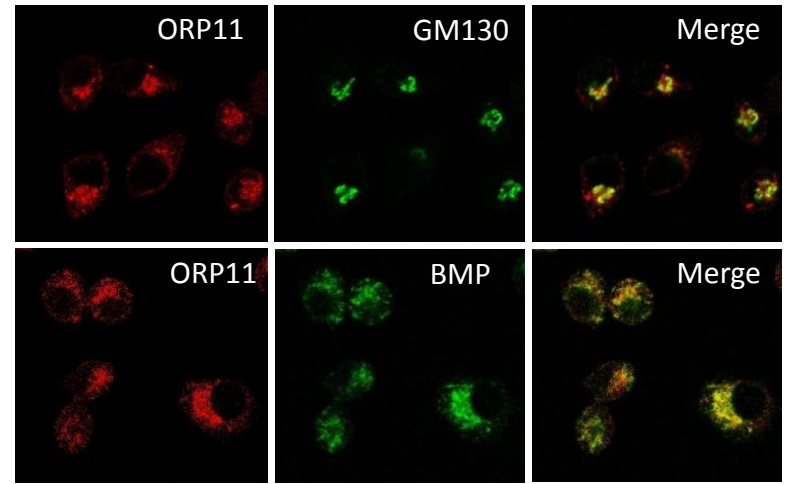


Figure 2



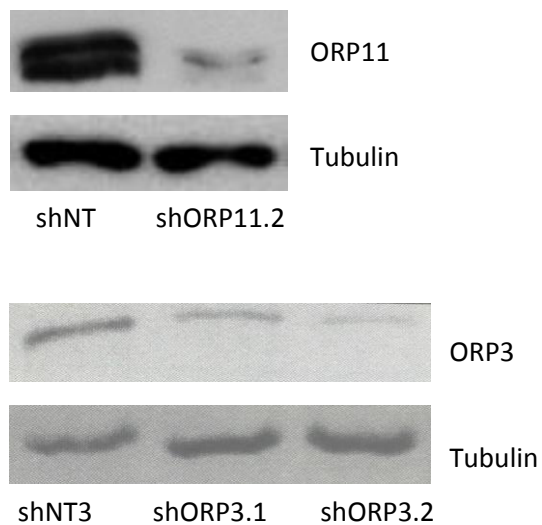
**B**



M1 and M2 colocalization values (ImageJ JACoP)	ORP11-GM130	ORP11-BMP
M1	0,67 ± 0,04	0,74 ± 0,02
M2	0,89 ± 0,03	0,91 ± 0,05

Figure 3

A



B

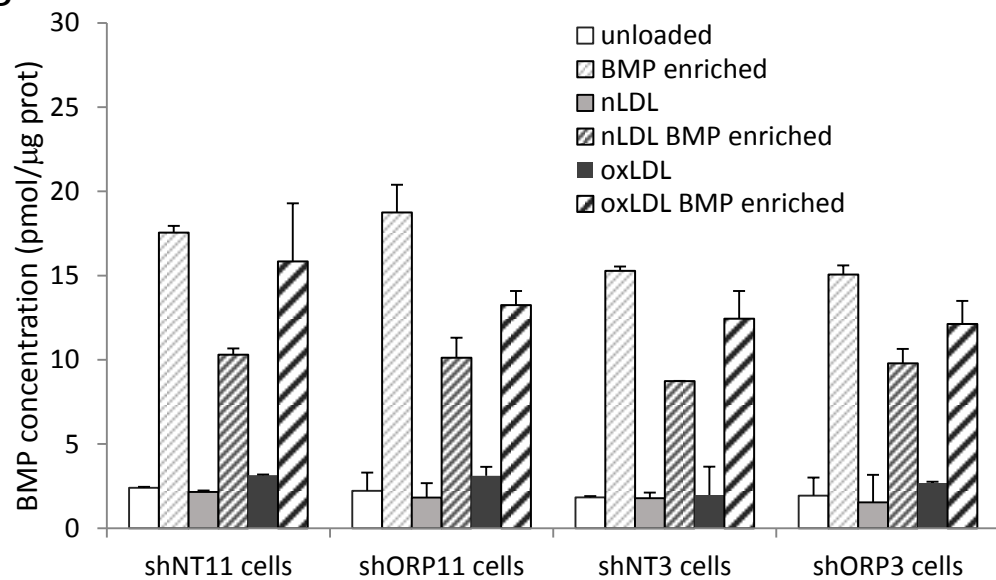


Figure 4

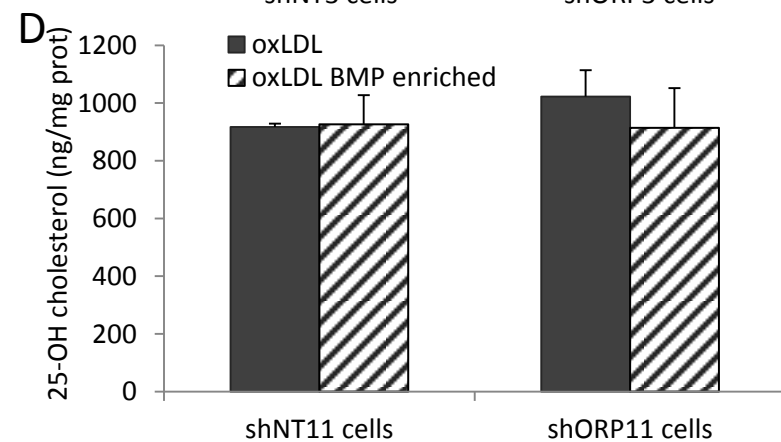
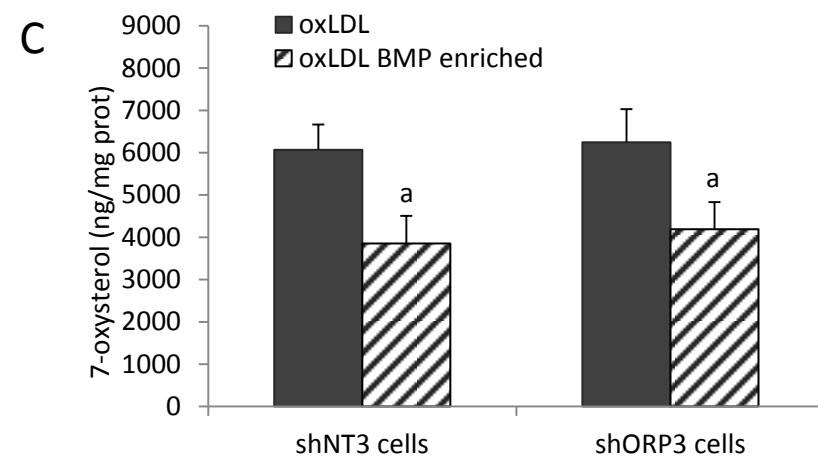
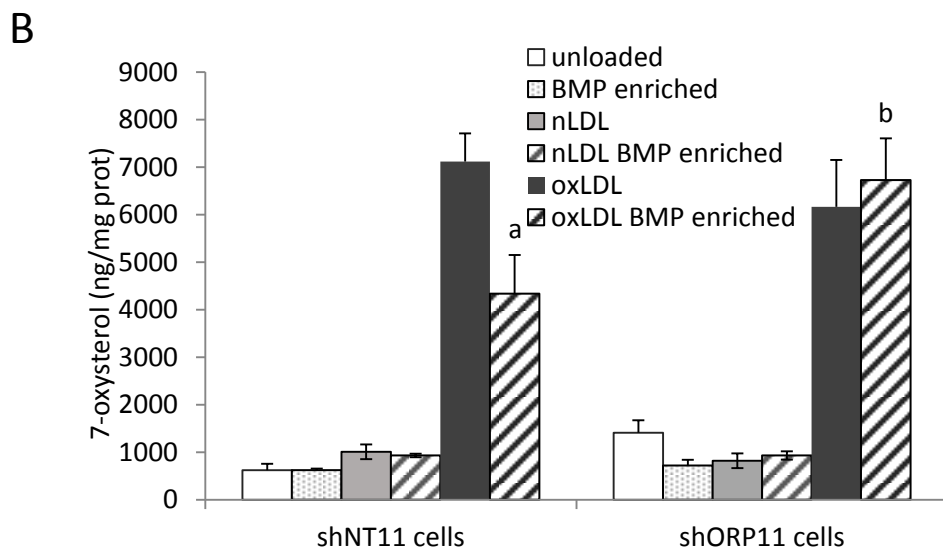
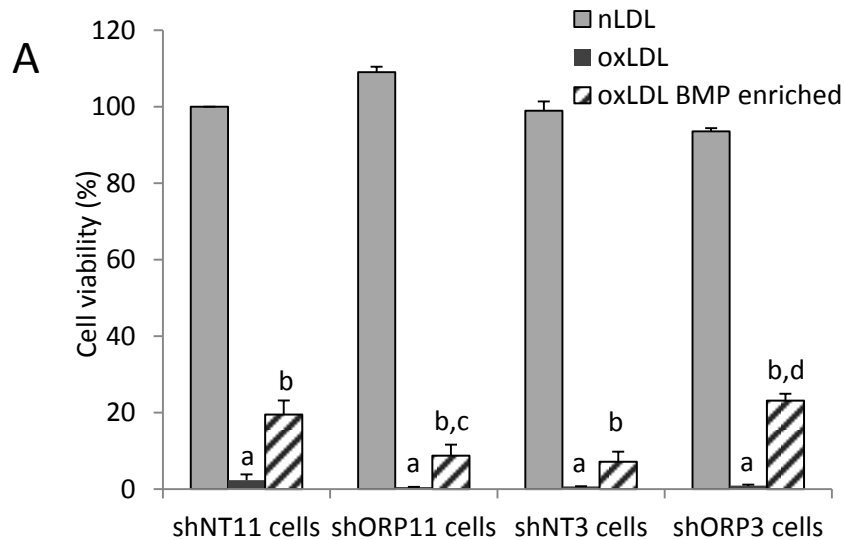
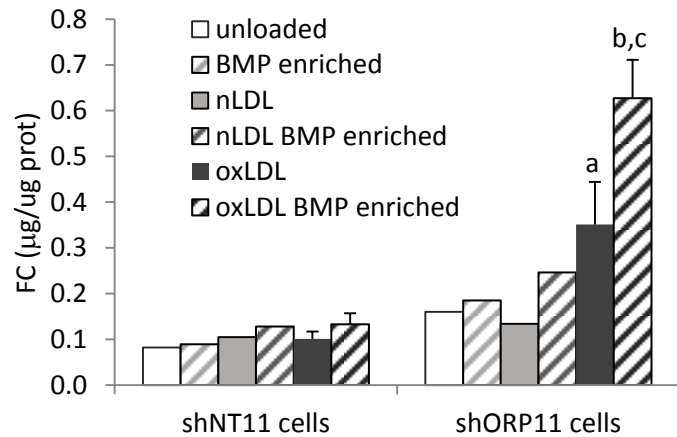
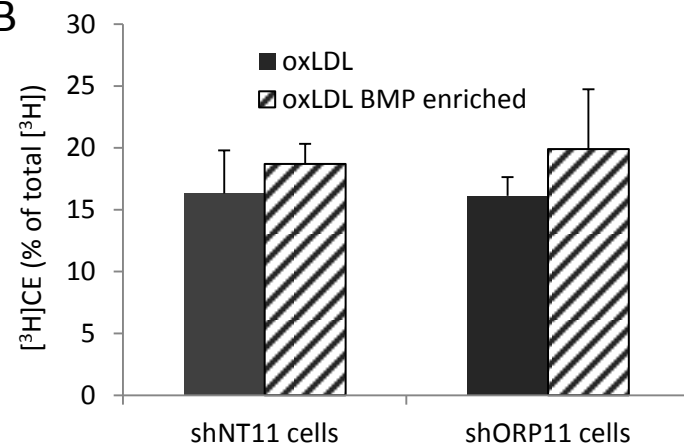


Figure 5

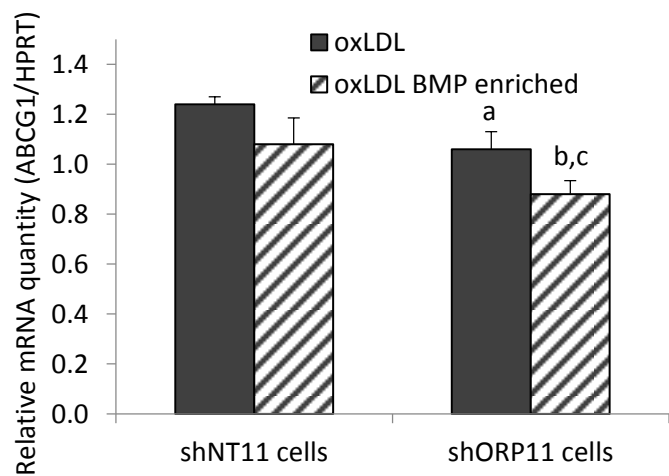
**A**



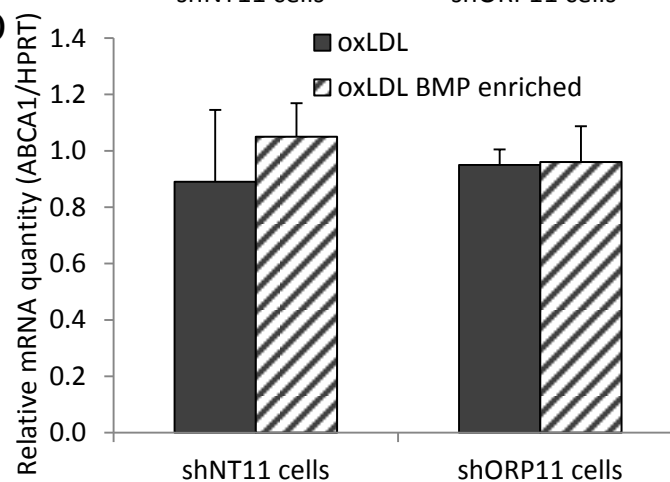
**B**



**C**



**D**



**E**

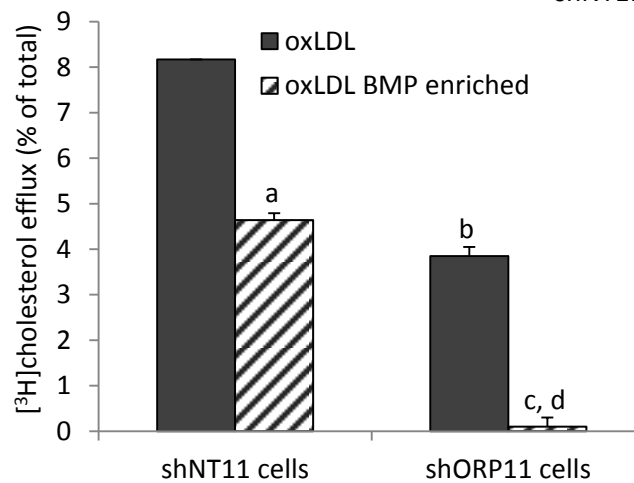


Table 1

BMP molecular species	shNT11 cells		shORP11 cells		shNT3 cells		shORP3 cells	
	18:1/18:1	18:1/18:1	18:1/18:1	18:1/18:1	18:1/18:1	18:1/18:1	18:1/18:1	18:1/18:1
	PG	PG	PG	PG	PG	PG	PG	PG
	mol%	oxLDL mol %	mol%	oxLDL mol %	mol%	oxLDL mol %	mol%	oxLDL mol %
16:0/18:1	4.21	6.63	2.56	5.68	2.99	5.83	2.36	7.25
18:1/18:2	4.38	14.05	3.23	13.74	4.32	12.59	5.39	12.74
18:1/18:1	72.73	66.88	80.47	69.77	73.55	65.97	65.74	58.83
18:2/18:2	0.00	0.39	0.00	0.41	0.01	0.30	0.00	0.40
18:1/20:4	1.75	1.99	1.82	2.17	2.27	3.07	2.12	2.64
18:2/20:4	0.01	0.09	0.01	0.07	0.03	0.10	0.01	0.21
18:1/22:6	16.00	9.24	10.87	7.44	13.75	10.20	20.33	14.83
18:1/22:5	0.92	0.74	1.04	0.73	3.08	1.96	4.06	3.10